



## **Chapter 4**

# **Materials and Experimental Methods**

## **Abstract**

The agricultural and industrial waste bio-mass samples were collected from local sources prepared for further analysis. The characterization of biomass samples was done by carrying out their proximate and ultimate analyses, evaluation of HHV, and percentage of cellulose, hemicellulose and lignin. The TGA and DTG analyses of all samples were carried out using a TGA/DTGA unit. The resultant data were analyzed using iso-conversional model free and model based methods. Batch pyrolysis of some selected biomasses were also carried out using a temperature controlled fixed bed tubular reactor. The bio-char and bio-oil produced were collected and analyzed. This section presents the details of experimental and analytical techniques used for above purpose.

### **4.1 Biomass collection and sample preparation**

Samples of rice husk (RH), rice straw (RS), wheat straw (WS), sugarcane bagasse (SB), arhar stalk (AS) and banana trunk (BT) were collected from the agricultural farm of the Institute of Agricultural Sciences, Banaras Hindu University campus (25.2623° N, 82.9894° E), Varanasi, Uttar Pradesh, India. The sugarcane leaves (SCL) and peanut shells (PS) were collected from fields located in Lakhimpur Kheri district (26.90°N 81.30°E) of Uttar Pradesh, India. The sample of paper mill waste (PMW) was collected from M/s Yash Paper Limited, Faizabad, India, a sugar-cane bagasse based paper mill. The PMW comprise the rejects from the cleaning and screening processes of the sugar cane bagasse produced during the mechanical pulping. These were selected on the basis of their abundant availability in this part of North India.

Approximately 2kg of each biomass were collected and surface adhered dust particles, soil, and other visible contaminants were removed manually and by washing with tap and distilled water. The washed biomass samples were dried in sun under atmospheric conditions for 48h. The sun-dried biomass samples were further dried separately in an air oven (Universal Oven Model NSW-143(OUA-2)) at 105°C for 4 h. The dried samples were coarse ground in a Wiley Mill (Model 2, Arthur H. Thomas. Co. Philadelphia, USA) to produce powder samples of uniform particle size.

The ground biomass samples were sieved into different particle size ranges: > 0.710, 0.710-0.600, 0.600-0.500, 0.500-0.425, 0.425-0.355, 0.355-0.300, 0.300-0.250, 0.250-0.180, and < 0.180mm. The mass of particles in each size range was determined and divided by the total mass of the biomass material to obtain the particle size distribution. The bulk density of each biomass for the particle size range of 0.185- 0.250 mm was determined as per ASTM 873 standard protocol. This fraction of each biomass was packed in separate airtight polyethylene bags and used in characterization and thermal degradation experiments. The photographs of the powdered sample of all the selected biomass are presented in Fig. 4.1.

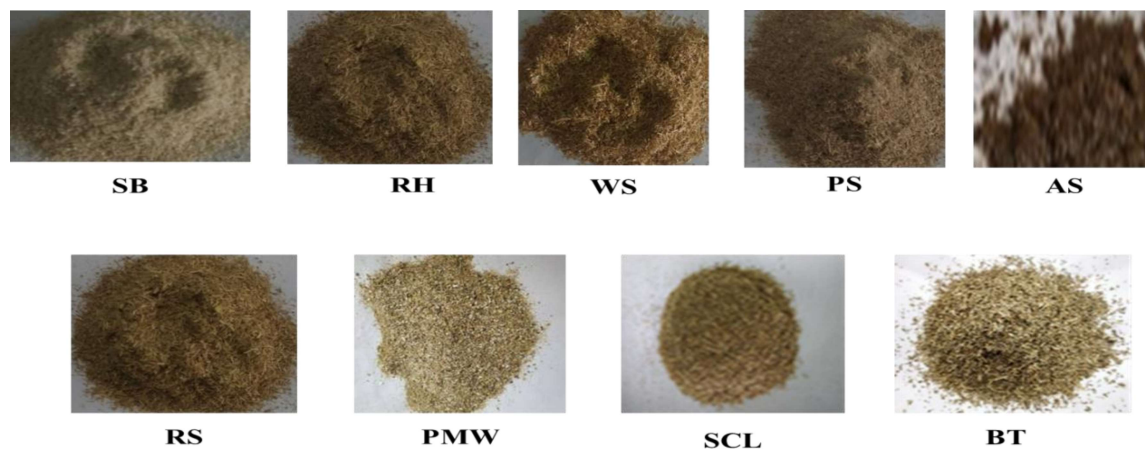


**Fig. 4.1** Photographs of selected biomasses

## 4.2 Biochemical and thermo-chemical characterization of raw biomasses

The lists of various thermo-chemical and biochemical procedures used for characterization of raw biomass are shown in Fig. 4.2.

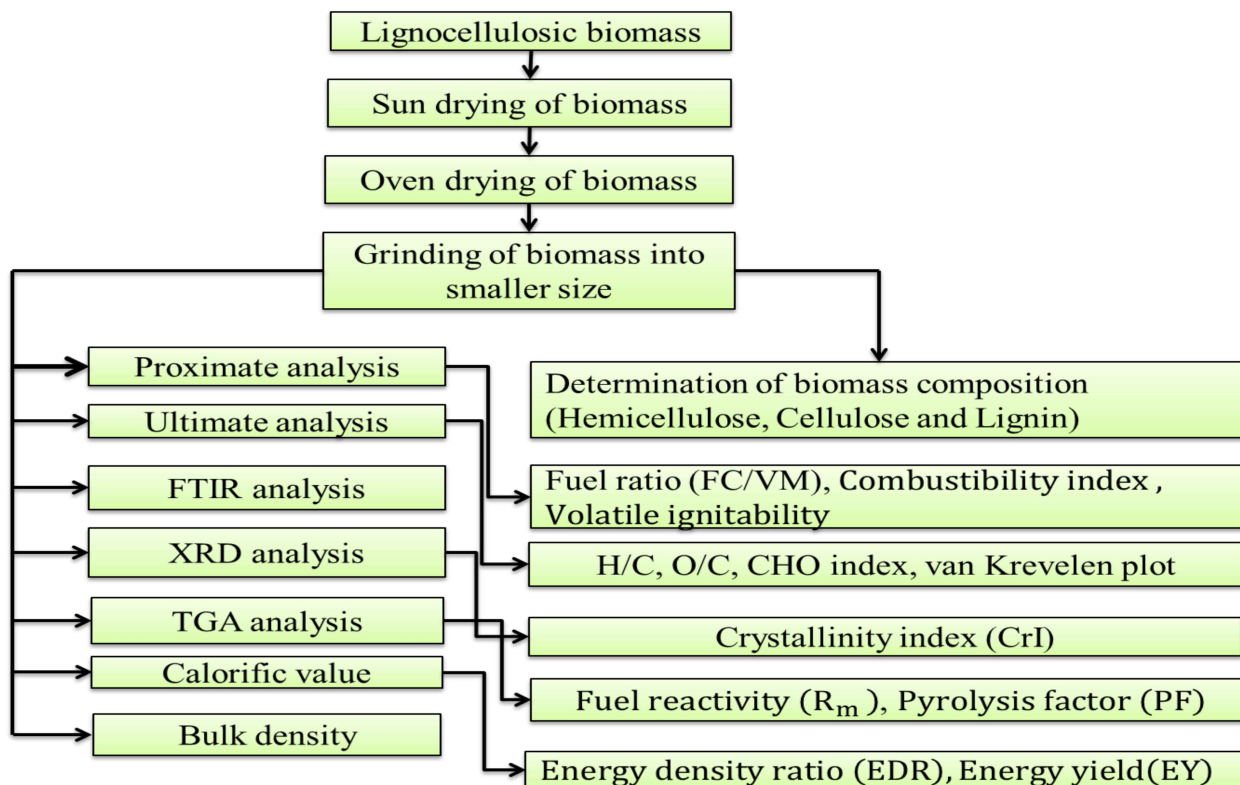


**Fig. 4.2** List of characterization techniques used for raw biomass samples characterization

## 4.3. Thermochemical characterization and thermal degradation studies

Thermo-chemical characterization of all the selected biomasses were carried out using proximate analysis (moisture content, volatile content, ash content and fixed carbon content), ultimate analysis, calorific value evaluation, thermogravimetric analysis (TGA), differential thermogravimetric (DTG) analysis, X-ray diffraction (XRD) studies, Fourier-

transform infrared (FTIR) spectroscopy and compositional analysis in terms of cellulose, hemicellulose and lignin.

#### **4.3.1 Proximate analysis**

The standard ASTM methods were adopted for the proximate analysis of all nine ground biomass samples between the sizes ranges (60 to 85-mesh).

##### **4.3.1.1 Moisture content**

For moisture content (MC) estimation 1g of the dried biomass sample was taken in a pre-dried silica crucible in a muffle furnace at a 105°C and heated for a period of 3h according to ASTM (E871-82, 2014). The crucible with sample was removed and allowed to cool to the room temperature in desiccators and re-weighed. The moisture content was calculated using the following formula.

$$MC (\%) = \frac{W_i - W_f}{W_0} \times 100 \quad (4.1)$$

where  $W_i$  represents the initial weight of sample plus crucible together,  $W_f$  represents the resulting dry weight of the crucible plus dry sample,  $W_0$  represents the initial weight of sample.

$$\text{Moisture free biomass (\%)} = 100 - \text{Moisture content (\%)} \quad (4.2)$$

##### **4.3.1.2 Ash content**

Accurately weighed 1g of the dried biomass sample was taken in a pre-weighed crucible and placed in a muffle furnace at 600°C for minimum 3h. The crucible was then removed and placed in a desiccator and cooled down to the room temperature. The crucible with ash

was weighed and placed back into the muffle furnace at the same temperature. This step was repeated until it attained a constant weight. The difference in weight was used to calculate the ash content in percentage. using the following formula (ASTM, 2013).

$$\text{Ash content (\%)} = \frac{A-B}{C} \times 100 \quad (4.3)$$

where A is the weight of crucible with ash, B is the weight of empty crucible, C is the weight of biomass sample taken for ash content.

#### **4.3.1.3 Volatile matter content**

According to ASTM D 3175-17, 1g of biomass sample was taken in a pre-weighed crucible with lid. After closing the lid, the crucible was placed in a muffle furnace at a temperature of 950°C for 7 min. The crucible was then removed carefully and placed in a desiccator to cool to the room temperature (ASTM D 3175-17). The crucible and its contents were reweighed and the loss in weight was used to calculate

$$\text{Volatile matter (\%)} = \frac{A-B}{A-C} \times 100 \quad (4.4)$$

where A is the weight of biomass sample with crucible and lid before heating, B is the weight of biomass sample with crucible and lid after heating, C is the weight of empty crucible with lid.

#### **4.3.1.4 Fixed carbon content**

The fixed carbon content (FC) was determined by the difference method (Balasundram et al., 2017):

$$\text{FC (\%)} = 100 - (\% \text{ Moisture content} + \% \text{ Ash content} + \% \text{ volatile matter}) \quad (4.5)$$

### 4.3.2 Ultimate analysis

The ultimate analysis or the elemental analysis of biomass sample was carried out by using a CHNS analyzer (Euro EA 3000, Elemental Analyzer, Riva Del Garda, Italy) to determine the percentage of carbon, hydrogen, nitrogen and sulfur content of the sample. The percentage of oxygen was calculated by the difference (Eshun et al., 2017; Balasundram et al., 2017).

### 4.3.3 Calorific value (Higher heating value)

The calorific value is the total amount of energy released when a unit mass or volume of fuel is entirely burnt in the presence of an excess supply of oxygen and is an indication of the energy content of any biomass material (Gravalos et al., 2016). It represents the how energy is released upon combustion of any biomass material (Mehmood et al., 2017). The calorific value (MJ/kg) measurement was carried out by pelletizing 1.0g of biomass sample and burning it in an automatic adiabatic bomb calorimeter (Digital bomb calorimeter, Model no.RSB 3, Rajdhani Scientific Instts.Co. New Delhi, India). The calorific value was calculated using the following formula.

$$CV = \frac{W * \Delta t - (CV_t + CV_w)}{m} \quad (4.6)$$

where W represents the water equivalent,  $\Delta t$  represents the rise in temperature,  $CV_t$  represents calorific the value of thread,  $CV_w$  represents the calorific value of wire and m represents the weight of the sample.

#### **4.3.4 van Krevelen plot**

The van Krevelen plot was drawn between the atomic ratio of hydrogen (H): carbon(C) to oxygen (O): carbon (C). It indicates the quantity of carbon-hydrogen and oxygen composition of any biomass material and relative position with respect to coal on this plot.

#### **4.3.5 Biofuel reactivity**

Biofuel reactivity is an important parameter for lignocellulosic biomass to be used for thermochemical conversion. It gives the information about reactivity of any biomass material for the optimum exploitation. Biofuel reactivity was estimated using proximate and ultimate analysis data. Reactivity was calculated by the atomic ratio of oxygen to carbon (O/C) and hydrogen (H/C) along with volatile matter to fixed carbon (VM/FC).

#### **4.4 Compositional analysis**

To determination of the component of lignocellulosic biomass and how it is distributed among (hemicellulose, cellulose, and lignin), the cellulose and hemicellulose were calculated by the procedure developed by Soest et al (1991) and the lignin by the procedure developed by Bledzki et al (2010). For determination of NDF, 1gm of thoroughly mixed biomass powder sample was taken in 500ml beaker and 100ml of neutral detergent solution with 0.5g of sodium sulfite was added. The beaker was put on the heating unit under the cold water condenser and refluxed for 60 min after the onset of boiling. The mixture was filtered and washed using 40ml boiling water then with acetone. The washed sample was dried at 105°C for overnight and its weight was recorded. The percentage NDF was calculated by the formula (Disco et al., 2017; Soest et al., 1991).

$$\text{NDF}\% = \frac{W_3 - W_1}{W_2} \times 100 \quad (4.7)$$

For acid detergent fiber (ADF) same procedure was employed as NDF, but the acid detergent solution was used in place of the neutral detergent solution, and percentage ADF was calculated as:

$$\text{ADF}\% = \frac{W_3 - W_1}{W_2} \times 100 \quad (4.8)$$

where  $W_1$  = Weight of empty filter paper,  $W_2$  = Weight of initial biomass sample,  $W_3$  = weight of fiber + filter paper.

For the determination of lignin content, 15 ml of 72% sulfuric acid was taken in a flask, and 2g of biomass sample was added. The mixture was stirred at room temperature for 3 hours and 200 ml of distilled water were then added, and the mixture was boiled for two hours and cooled. After 24 h, the lignin was washed with hot water and dried at 105°C and cooled down in a desiccator and weighed. The percentage of cellulose and hemicellulose was calculated as:

$$\text{Hemicellulose \%} = \text{NDF}\% - \text{ADF}\% \quad (4.9)$$

$$\text{Cellulose \%} = \text{ADF}\% - \text{Lignin}\% \quad (4.10)$$

#### 4.5 X-ray diffraction (XRD) pattern

The structural patterns (amorphous and crystalline) of biomass samples were determined using X-Ray diffraction system. The X-Ray diffraction patterns for the powdered biomass sample was collected using a X-ray diffraction unit (Rigaku Ultima IV, Rigaku Smart Lab 9 kW, Japan) with Cu  $K_\alpha$  radiation ( $\lambda=1.54\text{\AA}$ ) generated at 15 mA and a 40 kV unit was

used as the X-ray source. The X-ray diffraction patterns were recorded in a  $2\theta$  angle range of  $10-90^\circ$  at 298K with a scan speed of  $10^\circ/\text{min}$  and step width  $0.0200^\circ$ . Cellulosic material carries both crystalline (ordered) and amorphous (less ordered) phase. The relative amount of crystalline material in lignocellulosic biomass is indicated by the crystallinity index (CrI). The crystallinity index of biomass material was calculated by the following formula (Disco et al., 2017; Park et al., 2010):

$$\text{Crystallinity index (CrI)} = \frac{I_{002} - I_{AM}}{I_{002}} \times 100 \quad (4.11)$$

where  $I_{002}$  is the intensity at  $2\theta = 20$  for crystalline phase (cellulose) and  $I_{AM}$  is the intensity at  $2\theta = 16.6$  for the amorphous phase (cellulose, hemicellulose, lignin).

#### **4.6 Fourier-transform infrared (FTIR) spectroscopic analysis**

The FTIR spectroscopic analysis reflects the chemical functional groups present in the biomass sample. The Fourier-transform infra-red (FTIR) spectrophotometer (NICOLET 5700 FTIR, Thermo-electron Cooperation Waltham, Massachusetts, USA) was used for the analysis. The raw biomass was ground into powdered form to reduce scattering losses and absorption band distortion. The powdered biomass was mixed with KBr and passed into a translucent pelletized disc to form pellets. The spectra were collected within the range of  $400-4000\text{cm}^{-1}$  wave number with a scan rate of 40 and step size of  $4\text{cm}^{-1}$ .

#### **4.7 TG and DTG analysis**

The thermal degradation of biomasses were carried out using a simultaneous thermal analyzer which combined a heat flux type DSC with a TGA (STA 8000&8500 Perkin Elmer Ltd; with a precision of temperature measurement  $\pm 0.1\text{K}$ , DSC sensitivity  $\pm 0.1\text{mW}$

and microbalance sensitivity  $\pm 0.1\mu\text{g}$ ), to obtaining the data of weight loss with time or temperature throughout the pyrolysis reaction. Almost  $10\pm 0.01\text{mg}$  of powdered biomass sample (60-85 mesh size) was placed into alumina ( $\text{Al}_2\text{O}_3$ ) crucible and kept to equilibrate at  $30^\circ\text{C}$  for 30min, then constantly heating from  $30^\circ\text{C}$  to  $1000^\circ\text{C}$  at  $10^\circ\text{C}/\text{min}$ . To avoid unwanted secondary reaction and oxidation of sample, nitrogen gas at a flow rate of  $20\text{ml}/\text{min}$  was used to create an inert environment into the pyrolysis reaction chamber. To ensure the reproducibility, each experiment was repeated at least twice. DTG data of biomass samples were obtained by TGA data using origin pro software.

#### 4.8 DSC analysis

Differential scanning calorimetry (DSC) experiment was carried out using (STA8000&8500 Perkin Elmer Ltd.). The DSC is an important instrumental technique to calculate the rate of change of enthalpy of pyrolysis reaction. Heat flow (mW) was measured with time or temperature during DSC analysis.

#### 4.9 Kinetic analysis of thermal degradation results

Variation of biochemical composition in the lignocellulosic biomass leads to its thermal degradation through a complex pyrolysis process. To understand the global reaction mechanism of biomass pyrolysis, the overall reaction can be represented as follows (Kumar et al., 2009).

*Biomass(solid)*



Non-isothermal iso-conversional methods were employed for the evaluation of kinetic triplets of biomass pyrolysis. The model free kinetics produce distinct kinetic triplet as a function of the temperature of conversion. In isoconversional methods, the heterogeneous (solid to volatiles and char) reaction rate equation can be given as (Poletto et al., 2012):

$$\frac{d\alpha}{dt} = K(T)f(\alpha) \quad (4.13)$$

where t is time (min),  $\alpha$  is conversion:

$$\alpha = \frac{m_0 - m_t}{m_0 - m_\infty} \quad (4.14)$$

where  $m_0$  represents the initial weight of the sample,  $m_t$  represents sample weight at time t,  $m_\infty$  represents the final sample weight (solid residue) after decomposition.

In Eq. (4.13), the reaction rate ( $\frac{d\alpha}{dt}$ ) depends on the temperature dependent rate constant K (T) and reaction model function f ( $\alpha$ ). The rate constant K (T) can be expressed by using the Arrhenius type equation as follow:

$$K(T) = A \exp\left(\frac{-E_\alpha}{RT}\right) \quad (4.15)$$

where  $E_\alpha$  is apparent activation energy ( $\text{KJ mol}^{-1}$ ), A is a pre-exponential factor ( $\text{min}^{-1}$ ), T is the temperature in Kelvin (K), R is Universal gas constant ( $8.314 \text{ J/K.mol}$ ) and t is a time in min.

From Eq. (4.13) and Eq. (4.15) we get:

$$\frac{d\alpha}{dt} = A \exp\left(\frac{-E_{\alpha}}{RT}\right) f(\alpha) \quad (4.16)$$

The pyrolysis process reaction is temperature dependent, and the temperature is increasing with time at a constant heating rate, as the temperature is a function of time. A term heating rate  $\beta$  ( $^{\circ}\text{C}/\text{min}$ ) is introduced in Eq. 4.16 for the dynamic analysis of non-isothermal data obtained using TGA experiments as follows:

$$\beta = \frac{dT}{dt} = \frac{dT}{d\alpha} \frac{d\alpha}{dt} \quad (4.17)$$

$$\frac{d\alpha}{dT} = \frac{A}{\beta} \exp\left(\frac{-E_{\alpha}}{RT}\right) f(\alpha) \quad (4.18)$$

Integrating Eq. 4.18, for initial boundary condition,  $\alpha = 0$ , at  $T = T_0$  and after mathematical rearrangement gives the final equation as follows:

$$g(\alpha) = \int_0^{\alpha} \frac{d\alpha}{f(\alpha)} = \int_0^T \frac{A}{\beta} \exp\left(\frac{-E_{\alpha}}{RT}\right) dT \quad (4.19)$$

#### 4.10 Kinetic models for activation energy calculation

Integral iso-conversional methods were adopted for the kinetic modeling of biomass pyrolysis. According to Vyazovkin (2008), to find out the details of pyrolysis process of biomass using TGA data from multiple heating rates is more effective for activation energy calculation. For the constant heating rate of TGA data, Eq. 4.19 transform as follows

$$\begin{aligned} g(\alpha) &= \int_0^T \frac{A}{\beta} \exp\left(\frac{-E_{\alpha}}{RT}\right) dT \\ &= \frac{AE}{\beta R} P(x) \end{aligned} \quad (4.20)$$

$P(x)$  has no analytical solution; therefore, for all isoconversional methods, different mathematical approximations are used to solve the integral term. Kinetic models used for kinetic analysis of biomass pyrolysis are briefly discussed in the following section:

#### 4.10.1 Kissinger-Akahira-Sunose (KAS)

The KAS method is a very popular kinetic model among researchers for activation energy calculation of the pyrolysis process of biomass. First in 1956 Kissinger developed a kinetic model for activation energy calculation using TGA data. Later in 1971 Kissinger-Akahira-Sunose (Akahira and Sunose, 1971) used a mathematical assumption of  $P(x) = x^{-2}e^{-x}$  and the solution was expressed as follows:

$$\ln\left(\frac{\beta}{T^2}\right) = \ln\left(\frac{AE_\alpha}{Rg(\alpha)}\right) - \frac{E_\alpha}{RT} \quad (4.21)$$

For the constant value of a conversion ( $\alpha$ ), the activation energy of pyrolysis reaction was calculated using the slope of plot  $\ln\left(\frac{\beta}{T^2}\right)$  vs.  $1/T$ .

#### 4.10.2 Flynn Wall Ozawa (FWO)

Ozawa-Flynn-Wall (Ozawa, 1965; Flynn and Wall., 1966) used a mathematical expression for the exponential term known as Doyle approximation (Doyle, 1965) given as:

$$P(x) = -2.315 + 0.457x \quad (4.22)$$

Substituting Eq. (4.22) into Eq. (4.20) and solve to produce FWO equation which is expressed as follows:

$$\log(\beta) = \log\left(\frac{AE_\alpha}{Rg(\alpha)}\right) - 2.315 - 0.457\frac{E_\alpha}{RT} \quad (4.23)$$

where  $g(\alpha)$  is constant at a given value of the conversion. A linear relationship is observed by plotting  $\log(\beta)$  Vs.  $1/T$ . The slope of plot between  $\log(\beta)$  and  $1/T$  gives the values activation energy.

#### 4.10.3 Starink method

Starink developed a model for activation energy calculation which is similar to FWO and KAS. Value of activation energy calculated by Starink method is more precise than both the methods. Starink model described as follows (Starink, 2017):

$$\ln\left(\frac{\beta}{T^{1.92}}\right) = \text{Constant} - 1.0008\left(\frac{E_{\alpha}}{RT}\right) \quad (4.24)$$

The slope of plot between  $\ln\left(\frac{\beta}{T^{1.92}}\right)$  and  $1/T$  gives the value of activation energy at each conversion ( $\alpha$ ).

#### 4.10.4 Tang model equation

(Wanjuan et al., 2006) develop an equation for calculating activation energy. Tang equation expressed as follows:

$$\ln\left(\frac{\beta}{T^{1.894661}}\right) = C_1 - 1.001450\frac{E_{\alpha}}{RT} \quad (4.25)$$

The slope of plot between  $\ln\left(\frac{\beta}{T^{1.894661}}\right)$  and  $1/T$  gives the value of activation energy at each conversion ( $\alpha$ ).

#### 4.10.5 Friedman method

Friedman method is easy and most used for kinetic analysis and is different from the FWO, KAS, Starink, and Tang because it is a differential isoconversional method. In which no mathematical approximation and directly use to calculate activation energy by taking logarithm on both sides of using Eq. (4.16). The final Friedman equation can be described as follows:

$$\ln\left(\frac{d\alpha}{dt}\right) = \ln\left(\beta \frac{d\alpha}{dT}\right) = \ln[Af(\alpha)] - \frac{E_\alpha}{RT} \quad (4.26)$$

where  $\beta$  is the heating rate. The slope of the plot of  $\ln\left(\beta \frac{d\alpha}{dT}\right)$  vs.  $1/T$  gives the activation energy at each conversion ( $\alpha$ ).

#### 4.10.6 Vyazovkin method

It is the most accurate isoconversional method for activation energy calculation. In which no temperature integral approximation has been used. Vyazovkin (1997) defined a minimizing function as:

$$\Psi(E_\alpha) = \sum_i^n \sum_{j \neq i}^n \frac{I(E_\alpha, T_{\alpha,i})\beta_j}{I(E_\alpha, T_{\alpha,j})\beta_i} = \min \quad (4.27)$$

where  $I(E_\alpha, T_\alpha) = \int_0^{T_\alpha} \exp\left(\frac{-E}{RT}\right) dt$

The value of the activation energy was obtained by minimizing the function of Eq. (4.27) at a given conversion, when putting the experimental value of T and  $\beta$  into the equation. To

calculate the value of  $I(E_\alpha, T_\alpha)$  used numerical integration or 4th degree approximations were proposed by Senum and Yang (Senum and Yang, 1977) as follows:

$$I(E_\alpha, T_\alpha) = \frac{\exp(-x)}{x} \cdot \frac{x^3 + 18x^2 + 86x + 96}{x^4 + 20x^3 + 120x^2 + 240x + 120} \quad (4.28)$$

#### 4.10.7 Vyazovkin AIC (advanced isoconversional) method

This method is modified form of the Vyazovkin method and eliminates the drawback which is a disagreeable flattening of  $E_\alpha$  versus conversion ( $\alpha$ ). In which the temperature integral with limits  $T_{\alpha-\Delta\alpha}$  and  $T_\alpha(t_{\alpha-\Delta\alpha}$  and  $t_\alpha$ ) solved numerically by using trapezoidal rule (Mishra and Bhaskar, 2014). Vyazovkin AIC expressed model equation as follows (Vyazovkin, 2001):

$$J(E_\alpha, T(t)) = \int_{T_{\alpha-\Delta\alpha}}^{T_\alpha} \exp\left(\frac{-E}{RT(t)}\right) dt \quad (4.29)$$

$$\Psi(E_\alpha) = \sum_i^n \sum_{j \neq i}^n \frac{I(E_\alpha, T_i(t_\alpha))}{I(E_\alpha, T_j(t_\alpha))} = \min \quad (4.30)$$

In above equation  $T_i(t)$  ( $i=1 \dots n$ ) is the actual variations of temperature. Varying the value of  $E_\alpha$  in to Eq. (4.30) until the minimum value of function reached.

#### 4.10.8 Distributed activation energy model (DAEM)

The Distributed Activation Energy Model (DAEM) is an exact, adaptable and useful tool for evaluating the thermal degradation kinetics of various complex feedstocks (Arenas et al, 2019). It is a multi-reaction model that expects the degradation to happen through

countless independent, parallel, first or nth- order reactions with various activation energies (Cai et al., 2014; Wang et al., 2017). The DAEM expression can be represented (Ferdous et al., 2002; Miura and Maki, 1998) as:

$$1 - \frac{V}{V^*} = \int_0^\infty \exp\left(-A \int_0^t \exp\left(\frac{-E_\alpha}{RT}\right) dt\right) f(E) dE \quad (4.31)$$

where  $V^*$  and  $V$  represents the effective volatile and volatile content, respectively at temperature  $T$ ,  $f(E)$  represents the distribution functions of the activation energy.

The exponential terms in Eq. (4.31) approach to Eq. (4.32) (Gan et al., 2018) as:

$$\psi(E, T) = \exp\left(-\frac{A}{\beta} \int_{T_0}^T \exp\left(-\frac{E_\alpha}{RT}\right) dT\right) \approx \exp\left(-\frac{ART^2}{\beta E_\alpha} \exp\left(-\frac{E_\alpha}{RT}\right)\right) \quad (4.32)$$

A correlation between  $A$  and  $f(E)$  have been developed by Miura and Maki (1998), where  $\psi(E, T) = 0.58$  as:

$$-\ln(0.58) \frac{\beta C}{ART^2} = \exp\left(-\frac{E_\alpha}{RT}\right) \quad (4.33)$$

After simplifying Eq. (4.33), the simplified DAEM expression can be presented by Eq. (4.34) as:

$$\ln\left(\frac{\beta}{T^2}\right) = \ln\left(\frac{AR}{E_\alpha}\right) + 0.6075 - \frac{E_\alpha}{RT} \quad (4.34)$$

The values of  $E_\alpha$  and  $A$  can be calculated using the values of slope and intercept of the plot between  $\ln\left(\frac{\beta}{T^2}\right)$  versus  $\left(\frac{1}{T}\right)$  respectively at each conversion ( $\alpha$ ).

#### 4.11 Coats Redfern method

Thermogravimetric data has been used to elucidate the kinetic parameters (activation energy and pre-exponential factor) of solid state reactions. These parameters are useful to understand the thermal conversion processes of pyrolysis. The thermal degradation process is non-linear in nature therefore it displays different stages of pyrolysis using different models (Sriram and Swaminathan, 2018). The global rate equation for the pyrolysis of solid biomass as the substrate of the reaction exhibits the relationship between temperature and rate of reaction and is expressed by Arrhenius relations as:

$$\frac{d\alpha}{dt} = K(T) \cdot f(\alpha) \quad (4.35)$$

where,  $\alpha$ ,  $t$ ,  $K(T)$  and  $f(\alpha)$  represents the degree of conversion, time (min), rate constant which is function of temperature and reaction models which is function of degree of conversion respectively. The degree of conversion can be defined as:

$$\alpha = \frac{m_0 - m_t}{m_0 - m_f} \quad (4.36)$$

The reaction rate constant can be defined using the Arrhenius laws as:

$$k(T) = A \exp\left(\frac{-E}{RT}\right) \quad (4.37)$$

Where E represents the activation energy (kJ/mol), A indicate the pre-exponential factor (1/min), R is the universal gas constant (8.314 J/mol.K). Combine Eq. (4.35) and (4.37) gives the expression as:

$$\frac{d\alpha}{dt} = A \exp\left(\frac{-E}{RT}\right) \cdot f(\alpha) \quad (4.38)$$

In the above equation temperature is a function of time; therefore a term heating rate can be defined as:

$$\beta = \frac{dT}{dt} = \frac{dT}{d\alpha} \cdot \frac{d\alpha}{dt} \quad (4.39)$$

Putting the value of Eq. (4.37) in to the Eq. (4.36):

$$\frac{d\alpha}{dT} = \frac{A}{\beta} \exp\left(\frac{-E}{RT}\right) \cdot f(\alpha) \quad (4.40)$$

Integration of Eq. (4.40) from  $\alpha = 0$  to  $\alpha$  and  $T = 0$  to  $T$  gives:

$$g(\alpha) = \int_0^\alpha \frac{d\alpha}{f(\alpha)} = \frac{A}{\beta} \int_0^T \exp\left(\frac{-E}{RT}\right) dT \quad (4.41)$$

Equation (4.41) can be solved for activation energy and pre-exponential factors by using two approaches. First approach is the model free kinetic approach in which no reaction model is required and in the second approach a reaction model is required thus it is known as model fitting method.

The model fitting method was proposed first time in 1964 (Coats and Redfern, 1964) in order to investigate the reaction mechanism, activation energy and pre-exponential factor.

Solving the Eq. (4.41) for  $g(\alpha)$  gives:

$$g(\alpha) = \frac{ART^2}{\beta E} \left(1 - \frac{2RT}{E}\right) \cdot \exp\left(\frac{-E}{RT}\right) \quad (4.42)$$

Taking logarithmic of Eq. (4.42) and after rearrangement of Eq. (4.42) gives:

$$\ln\left(\frac{g(\alpha)}{T^2}\right) = \ln\left(\frac{AR}{\beta E}\right) \left(1 - \frac{2RT}{E}\right) - \frac{E}{RT} \quad (4.43)$$

The values of E would be sufficient high as well so the term  $2RT/E \ll 1$  can be neglected and Eq. (4.43) can be written as follows:

$$\ln\left(\frac{g(\alpha)}{T^2}\right) = \ln\left(\frac{AR}{\beta E}\right) - \frac{E}{RT} \quad (4.44)$$

Where  $g(\alpha)$  represent the integral reaction model. The slope and intercept of the plot between  $\ln\left(\frac{g(\alpha)}{T^2}\right)$  versus  $1/T$  gives the value of activation energy and pre-exponential factor respectively. The integral reaction mechanism models  $g(\alpha)$  are reported by Islam et al (2015) and Vyazovkin et al (2011).

#### 4.12 Multiple linear regression method

This method is different from isoconversional model free methods. It can be used for single heating rate and the entire temperature range to calculate the activation energy, pre-exponential factor, and order of reaction. Kinetic triplet (E, A, and n) using TGA data were calculated using the Arrhenius equation and methods describe (Kumar et al., 2008; Mansaray and Ghaly, 2015; Yin and Goh, 2015) as follows:

$$-\frac{dx}{dt} = Kx^n \quad (4.45)$$

$$-\frac{dx}{dt} = A \exp\left(\frac{-E}{RT}\right) x^n \quad (4.46)$$

where x represents the sample weight, K used for the reaction constant, n indicate the order of the reaction, A represents the pre- exponential factor, R shows universal gas constant, T

indicates absolute temperature and E is the activation energy of the reaction. Combining Eq. (4.45) and Eq. (4.46) gives equation.

$$\frac{-1}{m_0 - m_f} \frac{dm}{dt} = A \exp\left(\frac{-E}{RT}\right) \left(\frac{m_t - m_f}{m_0 - m_f}\right)^n \quad (4.47)$$

Integrating Eq. (4.47) and rearrangement of the resulting equation gives:

$$\ln\left(\frac{-1}{m_0 - m_f} \frac{dm}{dt}\right) = \ln(A) - \left(\frac{E}{RT}\right) + n \ln\left(\frac{m_t - m_f}{m_0 - m_f}\right) \quad (4.48)$$

where  $m_0$ =initial mass at the start of thermal decomposition,  $m_f$  = final mass at the end of thermal decomposition,  $m_t$  = mass at time t,  $dm/dt$  = rate of change of change mass. The Eq. (4.48) can be written in the linearized form of rate equation as follows:

$$y = B + Cx + Dz \quad (4.49)$$

where  $y = \ln\left(\frac{-1}{m_0 - m_f} \frac{dm}{dt}\right)$ ;  $x = 1/T$ ;  $Z = \ln\left(\frac{m_t - m_f}{m_0 - m_f}\right)$ ;  $B = \ln(A)$ ;  $C = \frac{-E}{R}$ ;  $D = n$ .

Value of B, C and D were calculated using TGA data at each heating rate in Microsoft excel which produces ANOVA analysis and subsequently calculates E, A, and n. The general procedure of analysis of the TGA data for evaluating kinetic parameters is shown in Fig 4.3. The summary of the various models is presented in Table 4.1

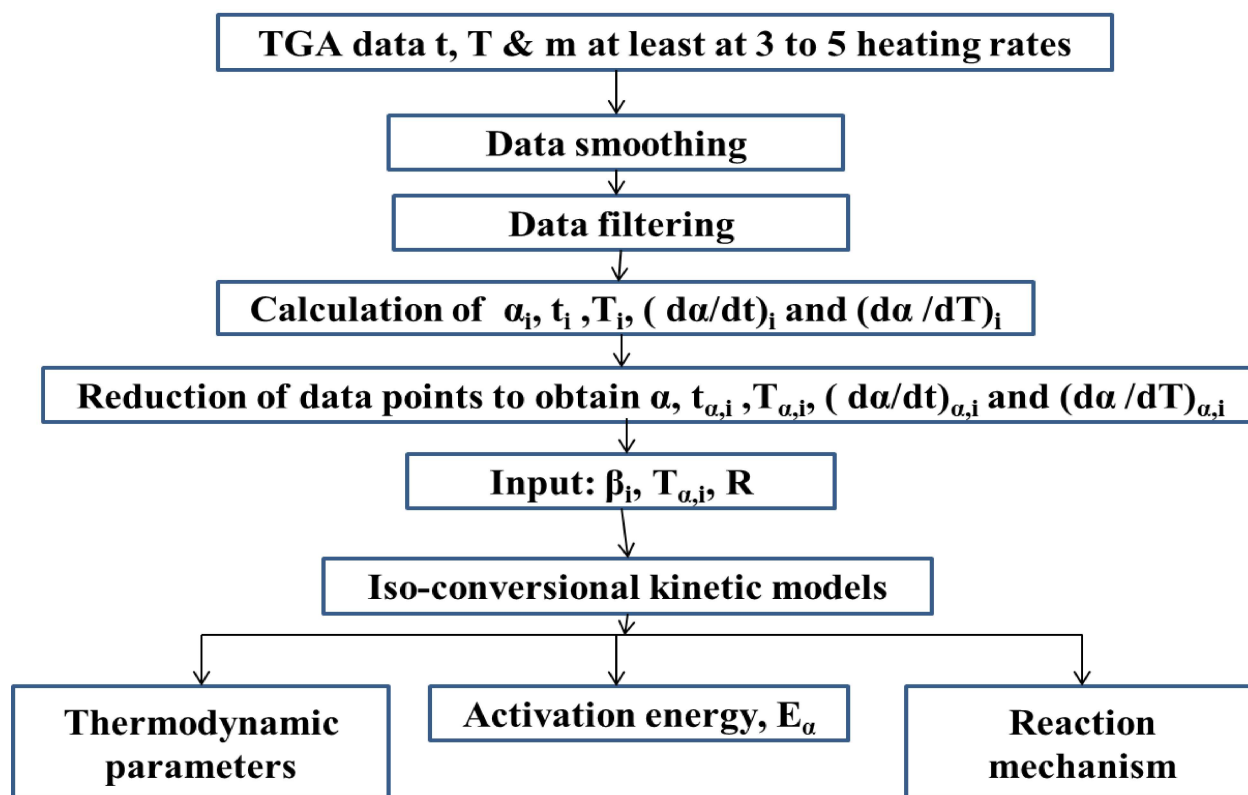


**Fig 4.3** General procedure for kinetic analysis of TGA data

**Table 4.1:** Available kinetic models for calculation of activation energy and pre-exponential factor

S. No.	Reference	Equation	Comments	Advantages & Disadvantages
	Flynn Wall Ozawa (FWO) method (Ozawa, 1965; Flynn and Wall., 1966)	$\log(\beta) = \log\left(\frac{AE_\alpha}{Rg(\alpha)}\right) - 2.315 - 0.457 \frac{E_\alpha}{RT}$	Used Doyel approximation, (Doyel, 1965), $P(x) = -2.315 + 0.457x$ , A plot of $\log(\beta)$ vs. $(1/T)$ is a straight line and its slope will give $E_\alpha$	i) It is linear method ii) it utilize oversimplified mathematical approximation for temperature integral iii) Significant error may observed in $E_\alpha$ iv) It is derived from the assumption of constant $E_\alpha$ from the

				beginning of the reaction to the end of the reaction
2	Kissinger-Akahira-Sunose (KAS) method (Akahira and Sunose, 1971)	$\ln\left(\frac{\beta}{T^2}\right) = \ln\left(\frac{AE_\alpha}{Rg(\alpha)}\right) - \frac{E_\alpha}{RT}$	Used mathematical assumption, $P(x) = x^{-2}e^{-x}$ for $\alpha = 0.05$ to $0.95$ , slope of plot of $\ln\left(\frac{\beta}{T^2}\right)$ vs. $1/T$ gives $E_\alpha$	<ul style="list-style-type: none"> <li>i) It is linear method</li> <li>ii) it utilize oversimplified mathematical approximation for temperature integral</li> <li>iii) Significant error may observed in <math>E_\alpha</math></li> <li>iv) It is derived from the assumption of constant <math>E_\alpha</math> from the beginning of the reaction to the end of the reaction</li> </ul>
3	Tang method (Wanjun et al., 2006)	$\ln\left(\frac{\beta}{T^{1.894661}}\right) = C_1 - 1.001450 \frac{E_\alpha}{RT}$	For conversion ( $\alpha$ ) $0.05 - 0.95$ , the slope of plot between $\ln\left(\frac{\beta}{T^{1.894661}}\right)$ and $1/T$ gives value of $E_\alpha$	<ul style="list-style-type: none"> <li>i) It is linear method</li> <li>ii) It is derived from the KAS method and more accurate than</li> </ul>
4	Starink method (Starink, 2017)	$\ln\left(\frac{\beta}{T^{1.92}}\right) = \text{Constant} - 1.0008 \left(\frac{E_\alpha}{RT}\right)$	The slope of plot between $\ln\left(\frac{\beta}{T^{1.92}}\right)$ and $1/T$ gives the value of $E_\alpha$ at each conversion ( $\alpha$ ).	<ul style="list-style-type: none"> <li>i) It is linear method</li> <li>ii) It is derived from the KAS method and more accurate than</li> </ul>
5	Friedman method (Friedman, 1964)	$\ln\left(\frac{d\alpha}{dt}\right) = \ln\left(\beta \frac{d\alpha}{dT}\right) = \ln[Af(\alpha)] - \frac{E_\alpha}{RT}$	Used without mathematical approximation, The slope of the plot of $\ln\left(\beta \frac{d\alpha}{dT}\right)$ vs. $1/T$ gives the activation	<ul style="list-style-type: none"> <li>i) It is linear methods of kinetics</li> <li>ii) It allow the linear variation of the heating rate</li> </ul>

			energy at each conversion ( $\alpha$ ) ranges from 0.05 to 0.95.	iii) It uses derivatives data of conversion. Consequently, leads to unstable and noise activation energy value
6	Vyazovkin method (Vyazovkin 1997)	$\Psi(E_\alpha)$ $= \sum_i^n \sum_{j \neq 1}^n \frac{I(E_\alpha, T_{\alpha,i}) \beta_j}{I(E_\alpha, T_{\alpha,j}) \beta_i}$ $= \min$ <p>where <math>I(E_\alpha, T_\alpha) = \int_0^{T_\alpha} \exp\left(\frac{-E}{RT}\right) dt</math></p>	The value of activation energy obtained by minimizing the function $\Psi(E_\alpha)$ , used numerical integration or 4th degree approximation were proposed by Senum and Yang for $I(E_\alpha, T_\alpha)$ (Senum and Yang, 1977; Pérez-Maqueda and Criado, 2000)	i) It is non-linear method ii) Not utilize any mathematical approximation for temperature integral iii) It is derived from the assumption of constant $E_\alpha$ from the beginning of the reaction to the end of the reaction iv) It is liable for less error for calculating activation energy
7	Vyazovkin AIC (advanced isoconversional) method (Vyazovkin, 2001)	$J(E_\alpha, T(t))$ $= \int_{T_{\alpha-\Delta\alpha}}^{T_\alpha} \exp\left(\frac{-E}{RT(t)}\right) dt$ $\Psi(E_\alpha)$ $= \sum_i^n \sum_{j \neq 1}^n \frac{I(E_\alpha, T_i(t_\alpha))}{I(E_\alpha, T_j(t_\alpha))}$ $= \min$	The temperature integral with limits $T_{\alpha-\Delta\alpha}$ and $T_\alpha(t_{\alpha-\Delta\alpha}$ and $t_\alpha$ ) solved numerically by using trapezoidal rule and varying the value of $E_\alpha$ until the minimum value of function reached.	i) It is non-linear method ii) Not utilize any mathematical approximation for temperature integral iii) It is derived from the assumption of constant $E_\alpha$ from the beginning of the reaction to the end of the reaction iv) It is liable for less error for calculating

				activation energy
				v) It is very accurate method
8	Multiple linear regression method (Kumar et al., 2008; Mansaray and Ghaly, 2015; Yin and Goh, 2015)	$\ln\left(\frac{-1}{m_0 - m_f} \frac{dm}{dt}\right)$ $= \ln(A) - \left(\frac{E}{RT}\right)$ $+ n \ln\left(\frac{m_t - m_f}{m_0 - m_f}\right)$	<p>where <math>m_0</math>=initial mass at the start of thermal decomposition, <math>m_f</math>=final mass at the end of thermal decomposition, <math>m_t</math> = mass at time t, <math>dm/dt</math>=rate of change of change mass</p> <p>It can be used for single heating rate and the entire temperature range to calculate the activation energy, pre-exponential factor, and order of reaction.</p> <p>Using TGA data at each heating rate in Microsoft excel which produces ANOVA analysis and subsequently calculates E, A, and n.</p>	<p>i) It is single heating rate method</p> <p>ii) it is most suitable for calculating straight line of TGA profile</p> <p>iii) it is less accurate method</p>
9	Coats-Red fern method (Damartzis et al., 2011)	$\ln\left\{\frac{1 - (1 - \alpha)^{1-n}}{T^2(1-n)}\right\}$ $= \ln\left\{\frac{AR}{\beta E}\right\} - \frac{E}{RT} \quad (\text{for } n \neq 1)$ $\ln\left\{\frac{-\ln(1 - \alpha)}{T^2}\right\}$ $= \ln\left\{\frac{AR}{\beta E}\right\} - \frac{E}{RT} \quad (\text{for } n = 1)$	<p>The kinetic plot between</p> $\ln\left\{\frac{1-(1-\alpha)^{1-n}}{T^2(1-n)}\right\}$ <p>versus <math>\frac{1}{T}</math> for <math>n \neq 1</math> and <math>\ln\left\{\frac{-\ln(1-\alpha)}{T^2}\right\}</math> versus <math>\frac{1}{T}</math> for <math>n = 1</math></p> <p>Gives slop <math>-\frac{E}{R}</math> and intercept <math>\ln\left\{\frac{AR}{\beta E}\right\}</math> to calculate order of reaction, pre-exponential factor and activation energy.</p>	<p>i) It is model-free method for calculating activation energy</p> <p>ii) mostly used for order of reaction and pre-exponential factor</p> <p>iii) It is single heating rate method</p>

10	Distributed activation energy method (DAEM) (Vand, 1943)	$\ln\left(\frac{\beta}{T^2}\right) = \ln\left(\frac{AR}{E}\right) + 0.6075 - \frac{E}{RT}$	<p>the plot between <math>\ln\left(\frac{\beta}{T^2}\right)</math> versus <math>1/T</math> gives a straight Line equation. <math>\frac{E}{R}</math> Provides slope of the equation; however, <math>\ln\left(\frac{AR}{E}\right)</math> provides intercept value while value 0.6075 kept constant for is simplicity.</p>	<p>i) It is in good agreement with experimental data, especially at low heating rates</p>
				ii)

#### 4.13 Determination of pre-exponential factor and reaction mechanism

The remaining parameter of kinetic triplets such as pre-exponential factor and reaction mechanism are evaluated using the Kissinger method and Criado method, respectively in this study. The activation energy of the pyrolysis process calculated using model free methods have been used for the reaction mechanism determination. Brief discussions of Kissinger and Criado methods are given below:

##### 4.13.1 Kissinger method for calculating pre-exponential factor

Kissinger proposed the first model for activation energy calculation in 1956. It is based on multiple heating rates and produces single activation energy for the entire pyrolysis process. Therefore, it is more suitable for calculating the pre-exponential factor (A). It has been used to calculate A (Chandrasekaran et al., 2017; Dhyani et al., 2017) are as follows:

$$\ln\left(\frac{\beta}{T_m^2}\right) = -\frac{E}{RT_m} + \ln\left(\frac{AR}{E}\right) \quad (4.50)$$

where  $T_m$  represent the peak temperature at a maximum conversion rate of the DTG curve. Pre – exponential factor (A) calculated using data of activation energy from model free methods at each conversion level and describe as follows:

$$A = \frac{\beta E \exp\left(\frac{E}{RT_m}\right)}{RT_m^2} \quad (4.51)$$

#### 4.13.2 Prediction of reaction mechanism: The z-master plot

Reaction mechanism of pyrolysis process has been investigated using Criado method (Criado et al., 1989) with the help of Z-master plot. In this approach, the shape of Z- master plot (theoretical plot) depends upon the reaction models. Thus, it is independent of the values of activation energy and pre-exponential factor. The expression for theoretical and experimental curves can be written as:

$$\frac{Z(\alpha)}{Z(0.5)} = \frac{f(\alpha) \times g(\alpha)}{f(0.5) \times g(0.5)} = \left(\frac{T_\alpha}{T_{0.5}}\right)^2 \times \frac{(d\alpha/dT)_\alpha}{(d\alpha/dT)_{0.5}} \quad (4.52)$$

Z-master curves were plotted using algebraic equations of different solid state reaction mechanism (Table 4.2). The plot between  $(Z(\alpha))/ (Z(0.5))$  and  $\frac{f(\alpha) \times g(\alpha)}{f(0.5) \times g(0.5)}$  gives the theoretical plot, while that between  $(Z(\alpha))/ (Z(0.5))$  and  $\left(\frac{T_\alpha}{T_{0.5}}\right)^2 \times \frac{(d\alpha/dT)_\alpha}{(d\alpha/dT)_{0.5}}$  gives the experimental plot. The possible reaction mechanism was found by comparing the theoretical and experimental plots.

#### 4.13.3 Prediction of reaction mechanism: Z-master plot

The reaction mechanism was predicted using Criado method proposed by (Criado et al., 1989) which is suitable for solid reaction processes and is given as follows:

$$Z(\alpha) = \frac{(d\alpha/dT)}{\beta} \times \Pi(x)T \quad (4.53)$$

where  $x = E/RT$  and  $\Pi(x)$  is a temperature integral approximation. Master plot are also known as theoretical plot which represents the reaction model, that is depends on conversion ( $\alpha$ ) only. The master curve was developed using various models given in Table 4.2. These theoretical plots were compared to experimental plot and determine the exact reaction mechanism which is a close fit to experimental plot. The experimental z-master plot was obtained using differential and integral forms of reaction model and is the given below:

$$Z(\alpha) = f(\alpha) \times g(\alpha) \quad (4.54)$$

$$Z(\alpha) = \frac{d\alpha}{dt} \exp\left(\frac{E}{RT}\right) \int_0^T \exp\left(\frac{-E}{RT}\right) \quad (4.55)$$

Temperature integral of Eq. (4.43) was solved using Senum-Yang approximation (Senum and Yang, 1977). Equation (4.54) was used for the theoretical plot and the experimental plot was obtained using Eq. (4.55)

$$Z(\alpha) = \frac{d\alpha}{dT} \frac{E}{R} \exp\left(\frac{E}{RT}\right) P(x) \quad (4.56)$$

**Table 4.2:** Algebraic expressions for  $g(\alpha)$  and  $f(\alpha)$  for the most frequently used common mechanisms operating in solid state reactions (Criado et al., 1989).

Reaction model	Code	Integral form $g(\alpha)$	Differential form $f(\alpha)$
<b>Nucleation and Growth</b>			
Avrami (Eq.1)	A <sub>1</sub>	$[-\ln(1 - \alpha)]^{2/3}$	$(3/2)(1 - \alpha)[- \ln(1 - \alpha)]^{1/3}$
Avrami (Eq.2)	A <sub>2</sub>	$[-\ln(1 - \alpha)]^{1/2}$	$2(1 - \alpha)[- \ln(1 - \alpha)]^{1/2}$
Avrami (Eq. 3)	A <sub>3</sub>	$[-\ln(1 - \alpha)]^{1/3}$	$3(1 - \alpha)[- \ln(1 - \alpha)]^{2/3}$
Avrami (Eq. 4)	A <sub>4</sub>	$[-\ln(1 - \alpha)]^{1/4}$	$4(1 - \alpha)[- \ln(1 - \alpha)]^{3/4}$
<b>Boundary Controlled Reaction</b>			
One-dimensional movement	R <sub>1</sub>	$\alpha^2$	$(1 - \alpha)$
Contracting area	R <sub>2</sub>	$(1 - \alpha)^{-1} - 1$	$(1 - \alpha)^2$
Contracting volume	R <sub>3</sub>	$(1/2)(1 - \alpha)^{-2} - 1$	$(1 - \alpha)^3$
<b>Diffusion Controlled</b>			
One-dimensional diffusion	D <sub>1</sub>	$\alpha^2$	$1/(2\alpha)$
Two-dimensional diffusion (Valensi model)	D <sub>2</sub>	$(1 - \alpha)\ln(1 - \alpha) + \alpha$	$[-\ln(1 - \alpha)]^{-1}$
Three-dimensional diffusion (Jander model)	D <sub>3</sub>	$[1 - (1 - \alpha)^{1/3}]^2$	$(3/2)(1 - \alpha)^{2/3}[1 - (1 - \alpha)^{1/3}]^{-1}$
Three-dimensional diffusion (GB model)	D <sub>4</sub>	$[1 - (2/3)\alpha] - (1 - \alpha)^{2/3}$	$(3/2)[(1 - \alpha)^{1/3} - 1]^{-1}$
<b>Random Nucleation</b>			
One nucleus on the individual particle	F <sub>1</sub>	$-\ln(1 - \alpha)$	$\alpha(1 - \alpha)$
Two nuclei on the individual particle	F <sub>2</sub>	$1 - (1 - \alpha)^{1/2}$	$2(1 - \alpha)^{1/2}$
Three nuclei on the individual particle	F <sub>3</sub>	$1 - (1 - \alpha)^{1/3}$	$2(1 - \alpha)^{2/3}$
<b>Power Law</b>			
Power law	P <sub>2/3</sub>	$\alpha^{3/2}$	$(2/3)\alpha^{-1/2}$
Power law	P <sub>2</sub>	$\alpha^{1/2}$	$2\alpha^{1/2}$
Power law	P <sub>3</sub>	$\alpha^{1/3}$	$3\alpha^{2/3}$
Power law	P <sub>4</sub>	$\alpha^{1/4}$	$4\alpha^{3/4}$

#### 4.14 Thermodynamic parameters

Values of activation energy calculated using various models (Table 4.1) have been used for thermodynamic parameters evaluation. Equation 4.57 through 4.60 have been used to evaluate the pre-exponential factor (A), enthalpy change ( $\Delta H$ ), Gibbs free energy change ( $\Delta G$ ) and entropy change ( $\Delta S$ ) respectively (Chong et al., 2019; Dhyani et al., 2017).

$$A = \beta E_{\alpha} \exp\left(\frac{E_{\alpha}}{RT_m}\right) / RT_m^2 \quad (4.57)$$

$$\Delta H = E_{\alpha} - RT \quad (4.58)$$

$$\Delta G = E_{\alpha} + RT_m \ln\left(\frac{K_B T_m}{hA}\right) \quad (4.59)$$

$$\Delta S = \frac{\Delta H - \Delta G}{T_m} \quad (4.60)$$

$K_B$  = Boltzmann constant ( $1.381 \ 9 \ 10^{-23}$  J/K),  $h$  = Plank constant ( $6.626 \ 9 \ 10^{-34}$  J s),  $T_m$  = DTG peak temperature.

The variation in values of  $E_{\alpha}$ , A,  $\Delta H$ ,  $\Delta G$  and  $\Delta S$  are used to compare the efficiencies of various models and ascertaining the ease of pyrolysis of biomass. Activation energy ( $E_{\alpha}$ ) plays an important role in the estimation of the reactivity of fuel. The reactivity of fuel plays an important role in pyrolysis processes. For assessing the fuel potential of a biomass thermodynamic parameters are also crucial for assessing the energy potential of biomass. The change in enthalpy ( $\Delta H$ ) indicates the absolute energy required by the biomass during pyrolysis. The change in Gibbs free energy ( $\Delta G$ ) uncovers the overall increment in the

energy of the system in the course of approachability of the biomass and formation of product.

#### 4.15 The batch pyrolysis experiments

For batch pyrolysis experiments a lab-scale experimental setup shown in Fig.4.4 was used. It is essentially a fixed-bed stainless steel tubular reactor (length: 520 mm; I.D. 44 mm) mounted inside an electrically heated vertical tube furnace. Approximately 20g accurately weighed sample was taken in each run. A constant flow of nitrogen gas (50mL/min) was maintained throughout the experiments to provide inert atmosphere and act as the carrier gas. The condensable vapors were collected in a bottle placed in an ice-bath. After attaining the set temperature, the heating was continued for additional 1h to collect all the condensable as liquid (bio-oil) and complete the char formation. The pyrolysis experiments were carried out in triplicate and average values (standard deviation of  $\pm 1.0$  %) are reported. The yields of pyrolysis product (condensed liquid, gas and bio-char) were calculated using the formula:

$$\begin{aligned} & \text{condensed liquid Yield (wt \%)} \\ &= \frac{\text{Bio oil (g)}}{\text{Biomass fed (g)}} \times 100 \end{aligned} \quad (4.61)$$

$$\text{Bio - char Yield (wt \%)} = \frac{\text{Bio char (g)}}{\text{Biomass fed (g)}} \times 100 \quad (4.62)$$

*Gas Yield (wt %)*

= 100

– {*Condensed liquid Yield (wt %) + B*

– *char Yield (wt %)*} (4.63)

*Conversion (%) = 100 – {Biochar yield (wt %)}* (4.64)

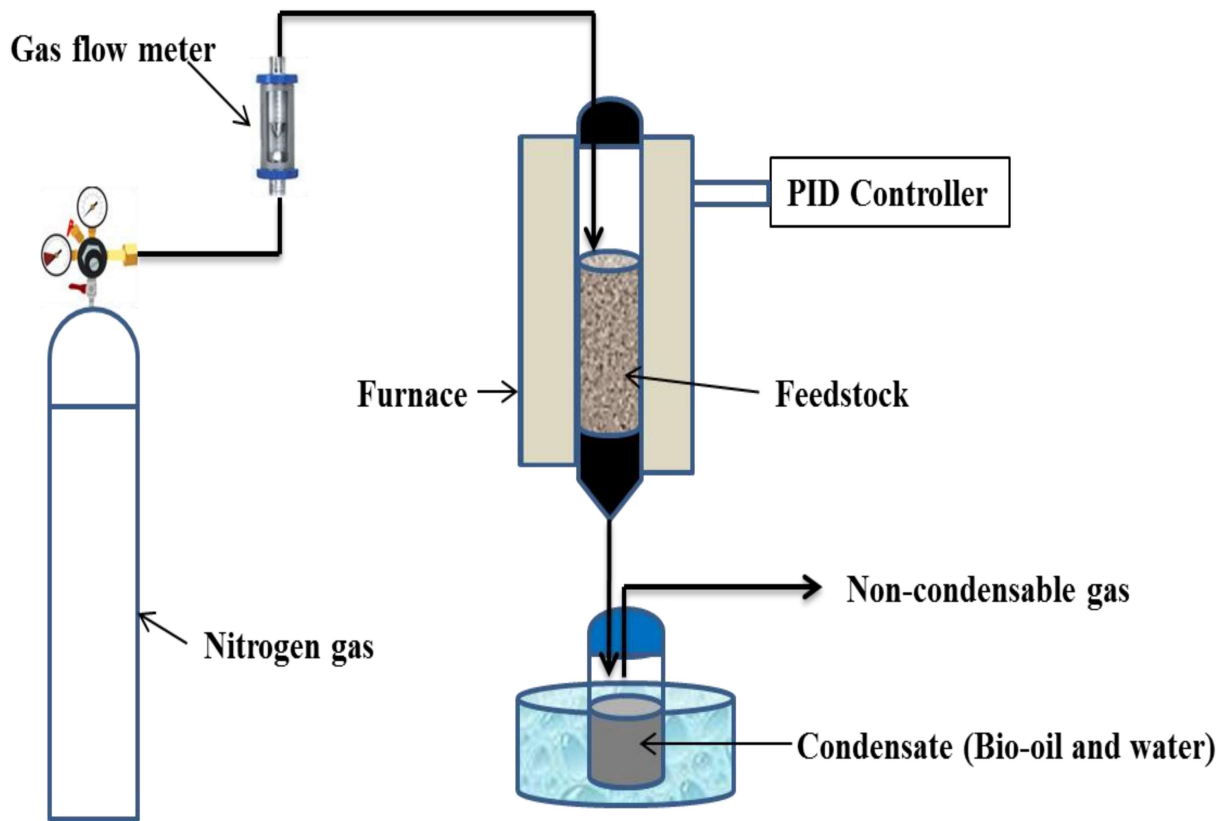


**Fig. 4.4** Block diagram of experimental setup for the batch pyrolysis

The results obtained through above experiments for the target biomasses are presented and discussed in following chapters.